Archives of Materials Science and Engineering

Volume 60
Issue 1
March 2013
Pages 24-31

International Scientific Journal
published monthly by the
World Academy of Materials
and Manufacturing Engineering

The lean duplex stainless steel welded joint after isothermal aging heat treatment

Z. Brytan [a,*], J. Niagaj [b]

[a] Division of Materials Processing Technology, Management and Computer Techniques in Materials Science, Institute of Engineering Materials and Biomaterials, Silesian University of Technology, ul. Konarskiego 18a, 44-100 Gliwice, Poland

[b] Institute of Welding, ul. Bł. Czesława 16/18, 44-100 Gliwice, Poland

* Corresponding e-mail address: zbigniew.brytan@polsl.pl

Received 29.01.2013; published in revised form 01.03.2013

ABSTRACT

Purpose: The purpose of this paper is the microstructural evaluation of the lean duplex stainless steel UNS S32101 (EN 1.4162) welded joints after isothermal aging heat treatment at 650°C. The scanning electron microscopy (SEM) and electron backscatter diffraction (EBSD) was applied in the microstructural analysis.

Design/methodology/approach: The welding joints were produced using the metal active gas (MAG) method where the filler metal was in wire form grade Avesta LDX 2101. During the process a shielding gas mixture of Ar + 2.5% CO_2 was applied and as a forming gas pure technical argon was used.

Findings: The welded joint in the as-welded condition shows Cr_2N nitride precipitation in the HAZ, while isothermal aging at 650°C for 15 min causes further precipitation of nitrides, both in the parent metal, as well as in the HAZ and the weld area. Increasing the aging time at this temperature to 90 min causes the formation of numerous nitrides at the grain boundaries of austenite and ferrite and nitride precipitation inside ferritic grains in each zone of the welded joint.

Research limitations/implications: The electron backscatter diffraction of particular zones of the welded joints considered only austenite and ferrite and their character was evaluated, while small precipitates like chromium nitrides were omitted in this study and will be evaluated in the further work.

Originality/value: Sometimes the production cycle involves the heat treatment of welded components made of lean duplex stainless steel. In such situations the additional heating of the welds and heat affected zone can produce carbides, nitrides or sigma phase precipitation - the extent of which depends on the temperature and time of heat treatment. These issues are widely reported in relation to the base material but not when considering welded joints, which may behave differently.

Keywords: Welding; Heat treatment; Lean duplex stainless steel; Chromium nitrides

Reference to this paper should be given in the following way:

Z. Brytan, J. Niagaj, The lean duplex stainless steel welded joint after isothermal aging heat treatment, Archives of Materials Science and Engineering 60/1 (2013) 24-31.

MATERIALS MANUFACTURING AND PROCESSING

1. Introduction

The recent developments in stainless steels are driven by two factors. The first factor concerns development of high resistant stainless steel grades for demand corrosion appliances. The result of such development in duplex grades is the hyper-duplex stainless steel grade (Fig. 1). This kind of grade (like UNS S33207) contains high Cr, Ni and Mo content, thus can be cost-effective alternatives to the super-austenitics or nickel-based alloys. The hyperduplex grades are characterized by excellent chloride corrosion resistance, combined with very high mechanical strength a currently are applied as seamless for tubes in subsea umbilicals to connect platform control stations and wellheads on seabed. The second approach is driven by the low cost of final material and such factor led to developments in the subgroup of lean duplex stainless steel. The main target is the development of lean duplex stainless steel with smaller alloying element content in respect to standard UNS S31803 (2205) duplex grade (22% Cr, 5% Ni, 3% Mo). The lean duplex stainless steel grade obtained through the decrease alloying element content is UNS S32304 (lower Ni content and lack of Mo). The second variety of lean duplex consists of grades with increased Mn content. The manganese replaces partially nickel, thus the austenite balance in duplex microstructure is maintained. This subgroup of lean duplex recently is developed. The standard grade of such alloys consists of UNS S32101 (21.5% Cr, 5% Mn, 1.5% Ni, 0.3% Mo,) that have successfully replaced standard austenitic grades in storage tanks and pressure vessels. This grade provides at least as good corrosion resistance in the sulphate liquor environment as standard chromium-nickel austenitic stainless steel, especially regarding to stress corrosion cracking. The mechanical properties of the lean duplex are more than twice higher, so the high reduction of thickness is possible. Evaluating the machinability of S32101 it is not more difficult to weld than standard austenitic grades, although higher forces are needed in forming operations due to higher strengths of duplex stainless family in general. The material cost of lean duplex grade S32101, even not lower than of the austenitic stainless steel it is characterized by high price stability due to considerably lower nickel content than in standard austenitic grades [1-5].

During the welding of duplex stainless steels the thermal cycle of welding can cause changes in the microstructure not only in the weld material, but also in the heat affected zone. These changes affect both the corrosion resistance of welded joints and their mechanical properties. Sometimes the production cycle involves the heat treatment of welded components or structures made of lean duplex stainless steel. In such situations the additional heating of the welds and heat affected zone can produce carbides, nitrides or sigma phase precipitation - the extent of which depends on the temperature and time of heat treatment. These issues are widely reported in relation to the base material but not when considering welded joints, which may behave differently because they posses initial microstructures that are different from that of the base material depending on the applied welding method, type of filler metal and the amount of heat input [6-19].

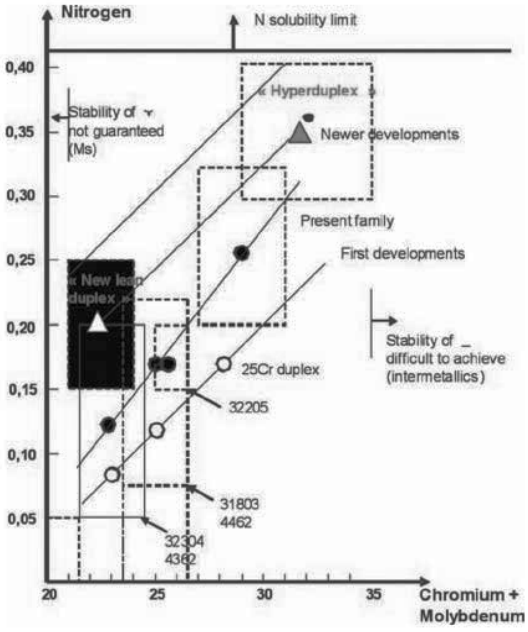

Fig. 1. Chemical composition of duplex stainless steel [4]

2. Experimental procedure

Lean duplex stainless steel, cold rolled and annealed sheet according to ASTM A240 S32101 (EN 1.4162) with a thickness of 6 mm was used for the study (Table 1). The welding joints were produced using the metal active gas (MAG) method where the filler metal was in wire form grade Avesta LDX 2101 with a diameter of 1.2 mm, as in Table 2. During the process a shielding gas mixture of Ar + 2.5% CO_2 was applied and as a forming gas pure technical argon according to standard EN ISO 14175-I1-Ar was used.

Table 1
Chemical composition of lean duplex stainless steel S32101

Grade	Chemical composition, wt %							
	C	Si	Mn	Cr	Ni	Mo	Cu	N
S32101	0.028	0.7	4.9	21.34	1.5	0.19	0.25	0.21

Table 2.
Chemical composition of wire electrode, 1.2 mm, grade AVESTA LDX 2101

Chemical composition, wt %									
C	Si	Mn	P	S	Cr	Mo	Ni	N	Cu
0.016	0.53	0.75	0.029	0.001	23.12	0.25	7.27	0.117	0.17

The welding joints were produced using mechanized welding stand consisting of a semi-automatic welding machine with synergistic control of Kemppi Pro 5200, a welding trolley DC20 PROMOTECH the precisely adjusTable travel speed of torch and an attachment device to position welded pieces. The shielding gas flow during MAG welding was adjusted between 14 and 16 l/min, while the forming gas was set to 5-6 l/min. The welding was

carried out using direct current with the positive end of the consumable electrode (DC +). The parameters of MAG welding for butt joints of 6 mm thickness made of lean duplex stainless steel S32101 are summarized in Table 3.

Table 3.
The MAG welding parameters of testing butt joints

Joint symbol	Number of beads	Welding current, A	Arc voltage, V	Welding speed, cm/min	Heat input, kJ/mm
6-20	1	116	22.6	9.2	1.368

After welding the test joints were subjected to heat treatment consist of aging at temperatures of 650°C for 15 and 90 min. in a neutral atmosphere.

Microstructure observations of welded joints were carried out using light and scanning electron microscopy. Light microscope observations involved etching using Aqua Regia reagent and were performed at 400x and 1000x magnifications using LEICA MEF4A microscope. The scanning electron microscope (SEM) involved in the studies was a SUPRA 25 of ZEISS Company equipped with an EDS probe. The SEM Inspect F with EBSD equipped with the automatic OIM (orientation imaging microscopy) software from TSL has been used to obtain more information about grain structure than optical microscopy. The samples for EBSD analysis were ground, polished with silicon carbide paper from grade 220 to grade 4000, and then with diamond paste (1 and 0.25 μm) on polishing clothes and finally argon-ion beam polished. The EBSD measurements were performed at 20 keV with a step size of 20 μm. The microstructural analysis was performed in the middle of the welded zone, around the root of weld, heat affected zone (HAZ) and in parent metal (Fig. 2) direction in the weld metal.

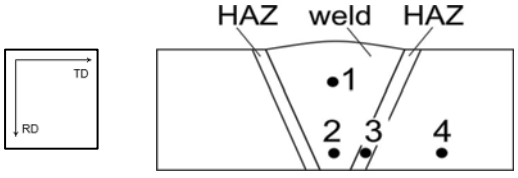

Fig. 2. The areas of microstructural studies in the welded joint and the arrangement of particular zones (1 - the weld, middle; 2 - the weld, root; 3 - the heat affected zone HAZ; 4 - the parent metal PM)

During SEM observations the EBSD analysis was applied in three different zones of each welded joint i.e. in the weld, HAZ and the parent metal. Crystal orientations maps (COM) were generated including the distribution of low- and high-angle boundaries, distribution of misorientation angles between all adjacent points, distribution of phases, grain size, grain size aspect ratio (defined as the minor axis of an ellipse divided by its major axis of a fitted ellipse, so a grain with a high aspect ratio has a needle-like shape), inverse pole figures for individual phases and the phase content in individual zones of the welded joint. The EBSD analysis was performed on the plane perpendicular to the welding direction of the transverse section of the weld, where the axis designation for EBSD, the (TD) axis corresponds to horizontal direction and (RD) axis correspond to a vertical direction (Fig. 1).

3. Experimental results and discussion

The welded joint of the S32101 grade in as-welded condition is characterized by a mixed distribution of both phases (ferrite and austenite) (Fig. 3). The ferrite content in delivery conditions in the parent metal according mill test certificate was 56% and measured be Fischer Feritscope FMP30 was 52%, giving medium about 53%, while measured on the surface was only 37%. The weld area shows higher austenite content about 70% that in the HAZ ca. 62% as well as in the parent metal. The weld microstructure is composed of a ferritic matrix where the austenite of different shape and orientation precipitated. The areas of intracellular austenite with characteristic trapezoidal and orthorhombic shape were also observed. Secondary phase precipitation has not been observed at grain boundaries of either phase. However in the HAZ, very numerous small precipitates, reported frequently in the literature [6, 8-10] as a chromium nitrides Cr_2N were observed in the ferrite grains and in ferrite/ferrite grain boundaries (Fig. 4). This phenomenon occurred only in the HAZ and its range does not exceed beyond this zone. The parent metal microstructure was free of secondary phase precipitation. The microstructure of the material in the weld area is characteristic for the welded duplex stainless steels with uneven distribution of both phases.

Analysing the chemical composition of ferritic and austenitic phase by the EDS analysis at as-welded conditions using the partition coefficient ($K_x=\alpha/\gamma$ weight %), the chemical composition in the weld zone shows very uniform distribution of alloying elements. The ferrite (α) is dominated by chromium, where $K_{Cr}=1.1$ and austenite (γ) is enriched in nickel and manganese and lower concentrations of Cr, where $K_{Mn}=0.81$ and $K_{Ni}=0.97$.

The precipitations of Cr_2N often reported in the welds of duplex stainless steels are found to precipitate in the intragranular ferritic regions (Fig. 4a) as well as in the boundaries of ferrite and austenite grains (Fig. 4b and 4c) where secondary austenite phase γ_2 visible as boundary thickening (Fig. 4c) precipitated with small nitrides of sharp shape inside of those regions. The mechanism of γ_2 precipitations studied by Ramirez [20,21] revealed that there are two different forms of such phase. The firs one form simply grows off the existing austenite and the other one form nucleates within the ferrite phase and is associated with previously precipitated chromium nitrides. According to this second precipitation mechanism the Cr_2N first nucleates at the inter-phase interface thus resulting in local depletion in chromium and molybdenum and in consequence this depletion leads the precipitation and growth of secondary austenite at the interface. The cooperative precipitation mechanism for growth of secondary austenite establish that the chromium nitrides precipitated at such interface will dissolve since they are isolated from the ferrite, what was also observed in studied case.

The heat treatment of the welded joint for 15 min at 650°C resulted in chromium nitrides Cr_2N precipitation beside the HAZ in the weld metal and in the parent metal (Fig. 5) in the form of intragranular precipitates in ferrite. During cooling from welding temperature the solubility of nitrogen in the ferrite drops and the ferrite becomes supersaturated in nitrogen, leading to the intragranular precipitation of needle-like Cr_2N and the same mechanism occurred during isothermal heating for 15 min in 650°C. The presence of another phase, like carbide or intermetallic phases was not revealed.

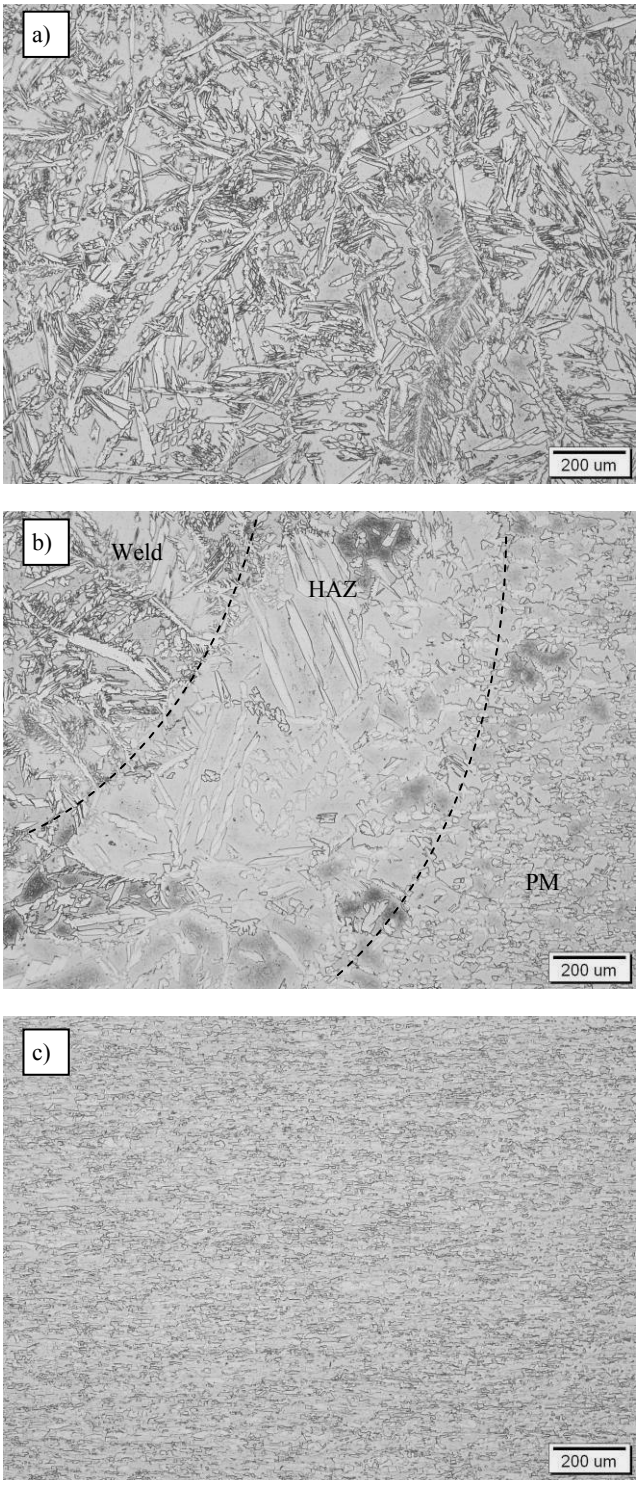

Fig. 3. The microstructure in as-welded conditions of lean duplex stainless steel S32101 in various zones, where a) the weld root (point 2 acc. to Fig. 1), b) HAZ (point 3 acc. to Fig. 1), c) parent material (point 4 acc. to Fig. 1), (Weld - the weld, the heat affected zone HAZ; the parent metal PM)

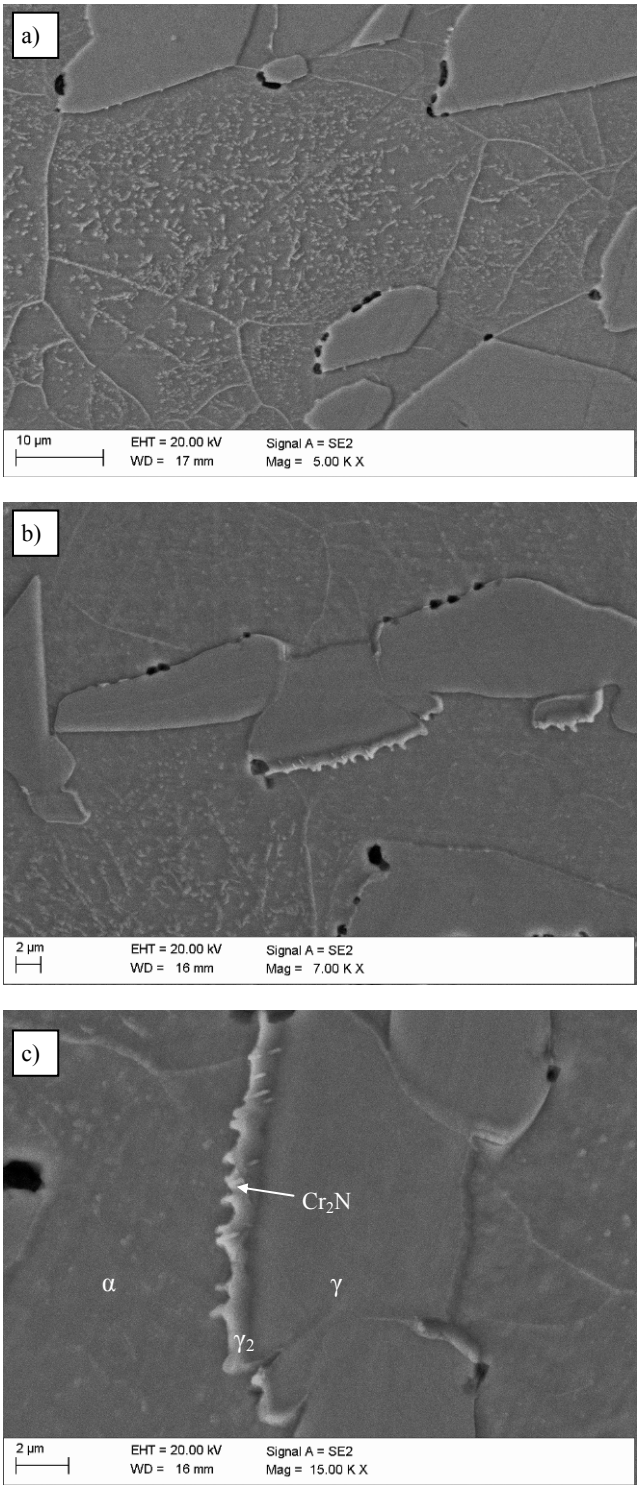

Fig. 4. The microstructure of lean duplex stainless steel S32101 of the welded joint in as-welded condition, evaluated by SEM, where in the HAZ a) small intragrannular precipitates of Cr_2N visible in the ferritic region, b) and c) the precipitates of Cr_2N on the boundaries of ferrite and austenite grain

Prolonged heating in the 650°C for 90 min resulted in the precipitation of the increased amount of the Cr_2N at the grain boundaries, which follows the cooperative precipitation of intergranular nitrides and γ_2 growth proposed by Ramirez [20].

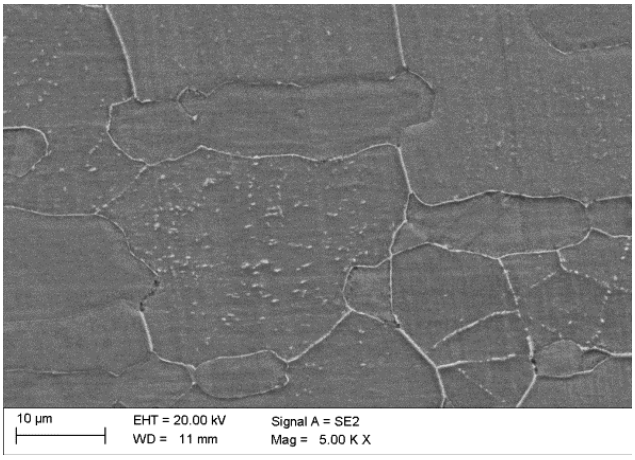

Fig. 5. The microstructure of the parent metal of the welded joint after aging at 650°C for 15 min

Figure 5a shows the intergranular precipitation of chromium carbides Cr_2N in the weld metal after isothermal heating at 650°C for 90 min, while Figure 6b the parent metal precipitates. According to some authors [7,8] similar precipitates were also identified like the carbides, but a very low amount of carbon in tested stainless steel as well as in applied filler metal exclude the carbide precipitation in the studied cases.

The presence of Cr_2N precipitations after isothermal aging of the welded joint are less harmful to mechanical properties, than precipitations of intermetallic sigma phase (σ), since its formation cause rapid deterioration in toughness and corrosion resistance of the duplex stainless steel [11]. The sigma phase precipitations occurs when the cooling rate during welding is not sufficient enough and the more highly alloyed alloys of the duplex stainless steel, the higher the probability of its formation. Therefore, hyperduplex and superduplex and standard 22%Cr duplex stainless steels are more prone to this problem than studied lean duplex stainless steel. The low amount of molybdenum in the parent metal as well as in the filler metal retard effectively precipitation of the sigma phase in the welded joints of lean duplex stainless steel, shifting the tendency to the sigma phase formation to prolonged aging time, exceeding analysed 90 min.

The sample after isothermal heating at 650°C for 90 min was studied also using the EBSD analysis, where the differences in the nature of austenite and ferrite in particular zones of welded joints were studied and existed small precipitates such as nitrides were not analysed (they will be studied in the future work). The phase content and grain boundary type in each zone of the welded joins is summarised in the Table 4. The austnite content increased from the parent metal to the weld providing expected toughness of the weld and proper phase balance in the duplex micostructure. The phase map in the parent metal, where the inverse pole figure of ferrite shows strong alignment to the <110> axes is shown in Figure 7. The inverse pole figure of austenite shows strong orientation of this phase between <111> and <001> axes.

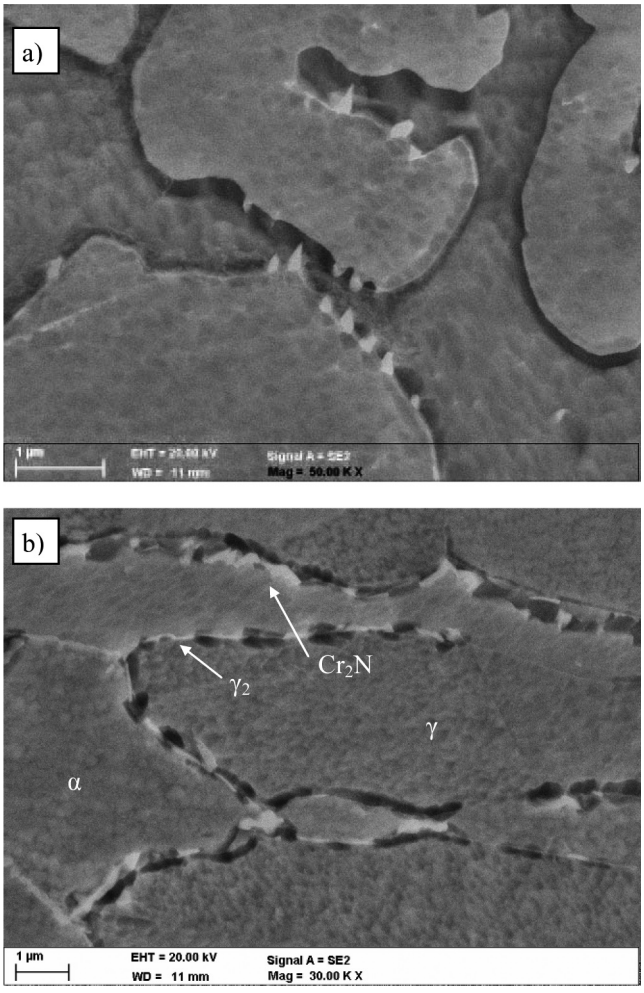

Fig. 6. The microstructure of the welded joint after aging at 650°C for 90 min, a) the weld metal, b) the parent metal

Table 4.
The phase content and grain boundaries tepe in particular zones of the welded joint

Zone of welded joint	Ferrite content (α), %	Austenite content (γ), %	Boundaries	
			Low angle (misorientation angle 2-15°)	High angle (misorientation angle 15-180°)
Parent metal	45	56	0.22	0.78
HAZ	40	60	0.13	0.87
Weld	37	63	0.16	0.84

The grain size and shape parameters are summarised in the Table 5, where the average grain size was estimated and the equivalent area of fitted ellipse. The gran size was estimated based on the fitted ellipse and its diameter and equivalent area, where the ellipse with minor and major axis represent shape aspect ratio. Moreover, the average grain shape was calculated by computing the average area and aspect ratio and then using a fitting approach to determine the angle between major axis to the horizontal. The grain

shape of individual grains was described by the major and minor axis of an equivalent ellipse. Calculated values refers to values excluding edge grains regions, where in the calculation points considered as the edge grains of particular phase were excluded.

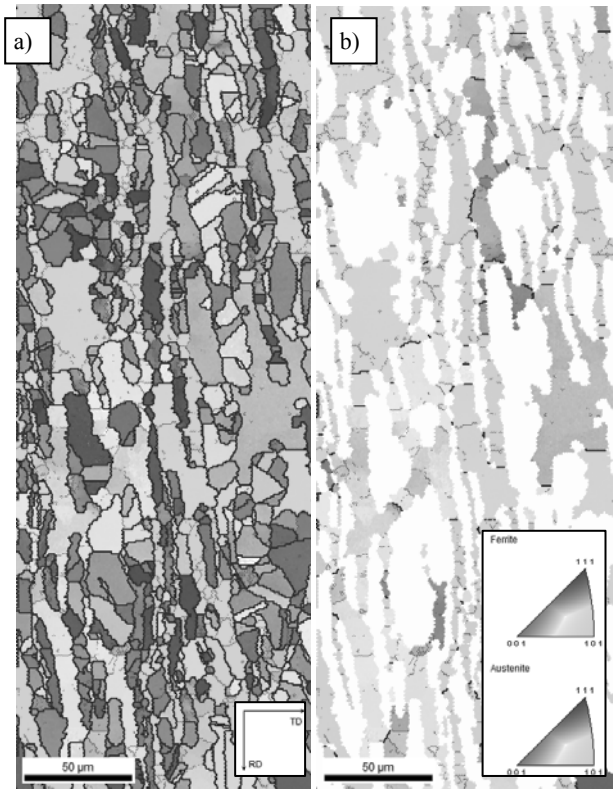

Fig. 7. The EBSD maps of the parent metal microstructure, a) the phase map and color coded map - inverse pool figure [001] of both phases, and b) of the ferrite, the color code is as follows: the red means a [001] crystal direction, blue a [111] direction, and green a [101] direction, respectively

Average grain size diameter of ferrite was calculated as 7.88 µm, where equivalent area of fitted ellipse was 48.81 µm^2 (Table 5).The major axis of ferrite in the parent metal was measured as 8.70µm, and minor axis as 3.40 µm, where the angle of major axis to the horizontal was 70.25 degrees. The ferritc phase in the parent metal shows predominantly low-angle boundaries, about 80% (the boundaries with misorientation angle in range 2-15°). The average grain size of austenite in the parent metal was smaller than that of ferrite. The average grain shape expressed by major axis of equivalent ellipse was 6.09 µm and the minor axis was 2.74µm, was smaller than for ferrite. The average grain size value of ferrite and austenite increased from the parent metal to the weld. Figure 8 shows the austenite grain size diameter in the weld and the parent metal, despite a slightly larger grain size of the austenite in the weld its size distribution shows greater irregularity due to specific character of resulting austenite in the weld. The grain shape aspect ratio of austenite in each zones of studied weld was in the range between 0.44 to 0.46, while for ferrite it was increased from 0.39 characteristic for parent metal to 0.51 in HAZ and 0.4 in the weld area.

Table 5.
The grain size and average grain shape of austenite and ferrite in particular zones of the welded joint after isothermal heating at 650°C for 90 min

Zone of welded joint	Phase	Grain size		Average grain shape			
		The average grain size, µm	Equivalent area, µm^2	Major axis, µm	Minor axis, µm	Grain shape aspect ratio	Angle to horizontal, degrees
Parent metal	α	7.88	48.81	8.70	3.40	0.39	70.25
HAZ		5.81	26.50	7.11	3.67	0.51	168.42
Weld		8.19	52.64	9.47	4.54	0.47	163.80
Parent metal	γ	7.31	41.91	6.09	2.74	0.45	15.97
HAZ		11.40	102.09	13.64	6.33	0.46	179.48
Weld		12.36	119.97	13.83	6.09	0.44	158.60

The EBSD analysis in the weld zone (Fig. 9) confirmed lower ferrite content in this zone, where the ferrite shows predominantly low-angle boundaries. Austenite contained both low- and high-angle boundaries, where high-angle boundaries was decreased comparing to parent metal and contained 56% of high-angle boundaries. The ferritic phase shows preferential grains orientation according to <001> direction (Fig. 9b), while austenite grains show mixed orientation. The austenite shows an increase in average grain size and three times increase of equivalent area of grain size (Table 5).

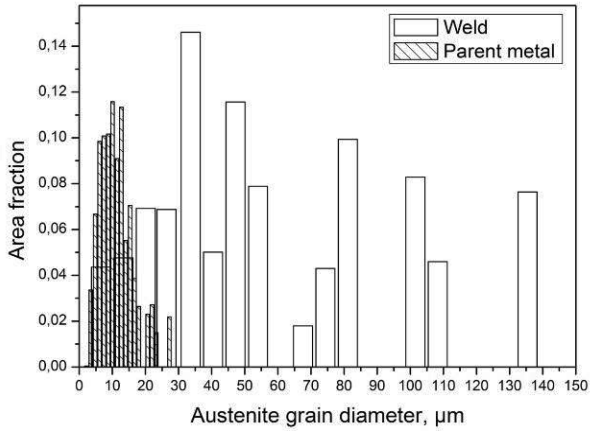

Fig. 8. The austenite grain size distribution in the weld and parent metal

The misorientation angle between adjacent austenite and ferrite boundaries in each zone of the welded joint were calculated. Figure 10 shows the distribution of the misorientation angle between austenite and ferrite boundaries for each studied zone. The misorientation angle between phases in the parent material lies preferentially near low angles below 5° and gradually increases near 40-45° and shows generally the random misorientation angle distribution (Fig. 10). The misorientation

angle between phases is fully different in the HAZ and the weld metal. The average grain misorientation angle between phases of lean duplex stainless steel welded joint in the weld metal and also in the HAZ lies near 40-45°, which contains both Nishiyama-Wassermann (N-W) and Kurdjumov-Sachs (K-S) crystallographic orientation relationships. The austenite phase can precipitate with near (N-W) or (K-S) orientation relationship. This result agrees with earlier results from the literature [18]. The (K-S) orientation relationships correspond to a 42.8° misorientation angle and (N-W) relationship to 45.9° so detailed analysis in this range was performed. This indicates that the orientation relationship between austenite and ferrite in the studied lean duplex stainless steel weld metal and HAZ is closer to the (N-W) orientation relationship than to the (K-S) one. The HAZ shows even slightly higher number of analyzed fractions that follows (N-W) orientation relationship than that in the weld zone.

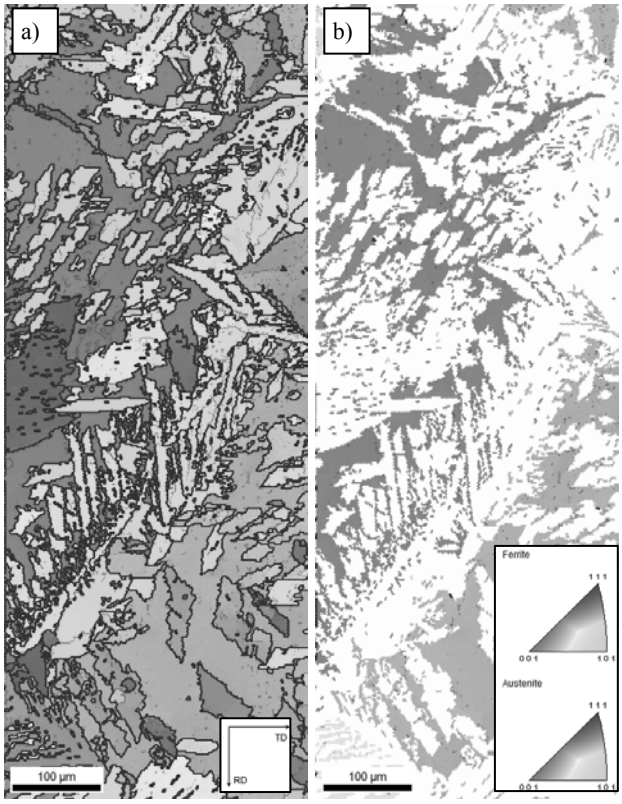

Fig. 9. The EBSD maps of the weld microstructure, a) phase map and color coded map - inverse pool figure [001] of b) ferrite and c) austenite, the color code is as follows: the red means a [001] crystal direction, blue a [111] direction, and green a [101] direction, respectively

The presence of such relationship between austenite and ferrite in the weld metal may influence on the easier propagation of dislocation slip from one phase to the other and then reduce the distribution of residual stresses [22] Presence of K-S relationship between austenite and ferrite was recently connected with lower ability to microcracks nucleation on the phase boundaries [23].

The high-angle boundaries are known to be cracking-susceptible boundaries. High-angle boundaries content for both phases was observed to reduce from the parent metal, over the HAZ into the weld, thus the crack initiated in the HAZ it cannot then readily propagate into the weld metal via such continuous, cracking-susceptible boundaries. The-high boundaries at austenite were decreased from 70% in parent metal to 52% in the HAZ and 56% in the weld. The low-angle boundaries that content increased in both phases in the weld metal shows ability to induce slip in neighboured grains thus reducing grain boundary stress and susceptibility for crack initiation.

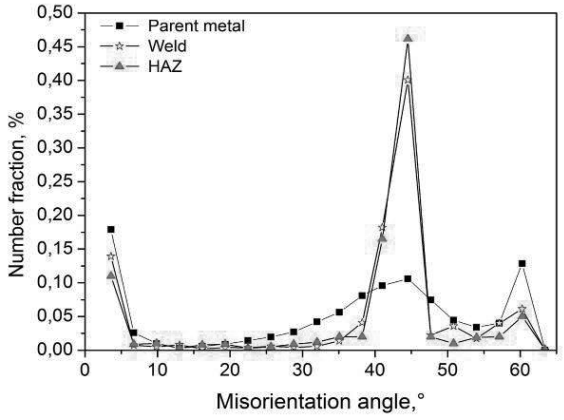

Fig. 10. The grain misorientation angle between austenite and ferrite in the parent metal the HAZ and the weld metal

4. Conclusions

The evolution of the S32101 (EN 1.4162) lean duplex stainless steel microstructure after welding and subsequent aging heat treatment has been investigated using SEM and EBSD analysis. The principal findings of this work are the followings:

1. The lean duplex stainless steel S32101 (EN 1.4162) welded joint in as-welded condition shows few Cr2N nitrides precipitations located only in the HAZ, while the parent metal an the weld are free of them.
2. The isothermal heat treatment at 650°C for 15 min causes formation of numerous chromium nitride precipitates, both in the parent metal, as well as in the HAZ and the weld area. Presented Cr_2N precipitates are mainly located as intragranullar precipitates in the ferritic regions.
3. The prolonged heat treatment at 650°C for 90 min causes the formation of nitrides precipitations predominantly located at the grain boundaries of both phases while intragranullar precipitates inside the ferrite grains were decreased. The precipitations on the grain boundaries were observed in each zone of the welded joint, in the weld, the HAZ and the parent metal.
4. The ferrite content decreased from 45% in the parent metal to 40% in the HAZ and 37% in the weld. The higher austenite content in the weld, closer to equilibrium, the optimal the mechanical properties of welded joints.

5. The crystallographic orientation relationships between neighbouring grains of austenite and ferrite observed during the EBSD analysis in the weld metal and the HAZ follows both Kurdjumov-Sachs (K-S) and Nishiyama-Wassermann (N-W) relationship favouring the (N-W) orientation relationships. The presence of such orientation relationship between austenite and ferrite in the weld metal and the HAZ together with the decrease of high-angle grain boundaries in both phases in the welded joint can make a contribution in reduction of present grain boundary stresses and decrease the susceptibility for crack initiation in the weld metal, thus increasing overall weld metal mechanical properties.

Acknowledgements

The authors gratefully acknowledge the financial support from the National Science Centre granted based on the decision number DEC-2011/01/B/ST8/06648.

The authors are grateful to Dr Klaudiusz Gołombek from Silesian University of Technology in Gliwice for his valuable support in SEM microstructural testing.

References

[1] Practical guidelines for the fabrication of duplex stainless steels, Published by IMOA, International Molybdenum Association, Second edition, 1999.
[2] G. Chai, U. Kivisakk, J. Tokaruk, J. Eidhagen, Hyper duplex stainless steel for deep subsea applications, Stainless steel world, 2009, 27-33.
[3] Duplex stainless steel LDX 2404™, Outokumpu stainless AB, Avesta Research Centre, 1447EN-GB:2 Centrumtryck AB, Avesta, Sweden, 2010.
[4] J.Ch. Gagnepain, Duplex stainless steels: success story and growth perspectives, Stainless steel world 12 (2008) 31-36.
[5] R. Gunn, Duplex stainless steels Microstructure, properties and applications, ISBN 1-85573-318-8, Abington Publishing, Cambridge, UK (1997).
[6] S. Baldo, K. Brunelli, I. Calliari, M.Dabala, L.Nordi, M.Zanellato, Characterization of lean duplex stainless steel, http://www.stainless-steel-world.net.
[7] H. Liu, P. Johansson, M. Liljas, Structural evolution of LDX 2101® (EN 1.4162) during isothermal ageing at 600-850°C, Proceedings of the 6th European Stainless Steel Conference, Science and Market, Helsinki, Finland, 555-560.
[8] Y.L. Fang, Z.Y. Liu, W.Y. Xue, H.M. Song, L.Z. Jiang Precipitation of secondary phases in lean duplex stainless steel 2101 during isothermal ageing, ISIJ International 50/2 (2010) 286-293.
[9] Z. Wei, J. Laizhu, H. Jincheng, S. Hongmei, Effect of ageing on precipitation and impact energy of 2101 economical duplex stainless steel, Materials Characterization 60 (2009) 50-55.
[10] B. Holmberg, M. Laren, Welding and applications of the new lean duplex steel LDX 2101, IIW Annual meeting, Prague, Czech Republic, 2005.
[11] Ch. Hsiehand, W. Wu, Overwiev of Intermettalic Sigma (σ) phase precipitation in Stainless Steel, International Scholarly Research Network, ISRN Metallurgy Article ID 732471, 2012.
[12] L. Karlsson, H.K.D.H. Bhadeshia, Some european developments in welding consumables, Journal of the Japan Welding Society 80/1 (2011) 110-119.
[13] J. Ćwiek, J. Łabanowski, S. Topolska, The effect of long-term service at elevated temperatures on structure and mechanical properties of Cr-Mo-V steel, Journal of Achievements in Materials and Manufacturing Engineering 49/1 (2011) 33-39.
[14] J. Nowacki, P. Rybicki, Influence of heat input on corrosion resistance of SAW welded duplex joints, Journal of Achievements in Materials and Manufacturing Engineering 17 (2006) 113-116.
[15] J. Nowacki, Ferritic-austenitic steel and its weldability in large size constructions, Journal of Achievements in Materials and Manufacturing Engineering 32/2 (2009) 115-141.
[16] S. Topolska, J. Łabanowski, Głowacka M, Failure of austenitic stainless steel tubes during steam generator operation, Journal of Achievements in Materials and Manufacturing Engineering 55/2 (2012) 378-385.
[17] S. Topolska, J. Łabanowski, Effect of microstructure on impact toughness of duplex and superduplex stainless steels, Journal of Achievements in Materials and Manufacturing Engineering 36/2 (2009) 142-149.
[18] J. Łabanowski, Mechanical properties and corrosion resistance of dissimilar stainless steel welds, Archives of Materials Science and Engineering 28/1 (2007) 27-33.
[19] J. Łabanowski, Stress corrosion cracking susceptibility of dissimilar stainless steel welded joints, Journal of Achievements in Materials and Manufacturing Engineering 20 (2007) 255-258.
[20] A.J. Ramirez, S. Brandi, J.C. Lippold, The relationship between chromium nitride and secondary austenite precipitation in duplex stainless steels, metallurgical Transactions 34A/8 (2003) 1575-1597.
[21] C. Lippold, D.J. Kotecki, Welding metallurgy and weldability of stainless steels, A Wiley-Interscience publication, 2005.
[22] R. Badji, T. Chauveau, B. Bacroix, Texture, misorientation and mechanical anisotropy in a deformed dual phase stainless steel weld joint, Materials Science and Engineering A 575 (2013) 94-103.
[23] I. Alvarez-Armas, M.C. Marinelli, J.A. Malarria, S. Degallaix, A.F. Armas, Microstructure associated with crack initiation during low-cycle fatigue in a low nitrogen duplex stainless steel, International Journal of Fatigue 29/4 (2007) 758-764.